Polydispersity-Driven Transition from the Orthorhombic *Fddd* Network to Lamellae in Poly(isoprene-*b*-styrene-*b*-ethylene oxide) Triblock Terpolymers

Adam J. Meuler,[†,§] Christopher J. Ellison,[†,§] Christopher M. Evans,[†] Marc A. Hillmyer,[*,‡] and Frank S. Bates[*,†]

Department of Chemical Engineering and Materials Science and Department of Chemistry, University of Minnesota, Minneapolis, Minnesota 55455

Received June 19, 2007
Revised Manuscript Received July 17, 2007

Most studies of block copolymers appearing in the literature have focused on macromolecules prepared by "living" anionic polymerization that are consequently comprised of nearly monodisperse ($M_w/M_n < 1.1$) blocks. While recent developments in synthetic techniques such as controlled radical polymerization (CRP) have increased the number of monomers that can be readily incorporated into block copolymers, materials with polydispersity indices exceeding 1.1 often result.[1] As a result, understanding the influence of polydispersity on the morphological behavior of block copolymers will become increasingly important.

The potential significance of polydispersity effects was pointed out more than 25 years ago by Leibler: "Much more important than fluctuation effects are those effects resulting from the polydispersity of the copolymer blocks. ...it seems that even a small polydispersity of the sample may be crucial."[2] Since then, numerous theoretical treatments have addressed the influence of polydispersity in AB diblock copolymers[3−7] and culminated in recent self-consistent mean-field theory (SCMFT) calculations.[8−11] The SCMFT calculations predict that the familiar lamellar, cylindrical, spherical, and gyroid morphologies persist over different composition regions depending on the constituent block polydispersities. Morphologies with larger mean interfacial curvatures are preferred with a polydisperse minority block while morphologies with smaller mean interfacial curvatures are favored when the polydisperse block is the major component. Theoretical treatments also predict that domain spacing and order−disorder transition temperature (T_{ODT}) will both increase with increasing polydispersity.

Relatively few experimental investigations of polydispersity effects have been undertaken. Early investigations by Matsushita and co-workers focused on blending nearly monodisperse poly(styrene-*b*-2-vinylpyridine) diblock[12,13] and poly(2-vinylpyridine-*b*-styrene-*b*-2-vinylpyridine) triblock[13,14] copolymers. These studies demonstrated the predicted increase in domain spacing with increasing polydispersity, but macrophase separation occurred when the molecular weight and/or composition were too disparate. Bendejacq et al. used CRP to synthesize poly(styrene-*b*-acrylic acid) diblocks with overall polydispersities near 2 and did not observe any macrophase separation, demonstrating an important difference between the multicomponent blends and a continuous molecular weight distribution.[15] Lynd and Hillmyer synthesized low molecular weight conformationally symmetric poly((ethylene-*alt*-propylene)-*b*-(DL-lactide)) with a monodisperse poly(ethylene-*alt*-propylene) block and a poly(DL-lactide) block ranging in polydispersity from 1.2 to 2.[9] The lamellar, cylindrical, and gyroid morphologies were observed, with interfacial curvature varying with polydispersity in general agreement with SCMFT predictions. Most recently, Ruzette and co-workers used nitroxide-mediated polymerization to synthesize AB diblock and ABA triblock copolymers consisting of poly(butyl acrylate) (B block) with a relatively narrow molecular weight distribution and relatively polydisperse poly(methyl methacrylate) (A block).[1] Lamellae, hexagonally packed cylinders, and poorly order spherical micelles were identified, and no macrophase separation was observed. Domain interfaces curved toward the polydisperse A block relative to the curvature expected for a monodisperse system, also in agreement with SCMFT predictions.

The aforementioned investigations of broad, continuous molecular weight distributions[1,9,15] focused on systems with two chemically distinct blocks where the polydisperse blocks have one chain end not constrained to a domain interface. This Communication describes the preliminary results of an investigation of poly(isoprene-*b*-styrene-*b*-ethylene oxide) (ISO) triblocks along the $f_I = f_S$ isopleth with nearly monodisperse polyisoprene (PI) and poly(ethylene oxide) (PEO) end blocks but a modestly polydisperse ($M_w/M_n = 1.31$ and 1.44) polystyrene (PS) middle block. The large value of χ_{IO} relative to χ_{SO} and χ_{IS} ($\chi_{IO} = 0.17$, $\chi_{IS} = 0.04$, $\chi_{SO} = 0.05$ at 120 °C)[16] should force bridging of the polydisperse PS block. The nearly monodisperse ISO system has already been extensively characterized,[17−19] facilitating isolation of the morphological effects of polydispersity in a bridged domain.

Two hydroxy-functionalized SI diblocks with a polydisperse PS block and a nearly monodisperse PI block were prepared by anionic polymerization in cyclohexane using the functional organolithium 3-triisopropylsilyloxy-1-propyllithium (TIPSOPrLi).[20] Adding styrene monomer to a solution of TIPSOPrLi over a very short time interval resulted in M_w/M_n values of 1.31 and 1.44, as generally expected.[20] Upon isolation of the SI diblocks, the TIPS protecting group was removed using tetra(*n*-butyl)ammonium fluoride (TBAF) to unmask the α-hydroxyl group. The ethylene oxide polymerization was initiated from this hydroxyl group using an established protocol.[21] The ISO triblocks were purified by dichloromethane/distilled water washes followed by precipitation in isopropanol and freeze-drying from benzene.

Room temperature size exclusion chromatography (SEC) experiments employing THF as the mobile phase were performed on a Waters 717 GPC, and data were calibrated with PS standards to determine the polydispersity of all polymers. Synchrotron small-angle X-ray scattering (SAXS) experiments were conducted at the Advanced Photon Source at Argonne National Laboratory using $\lambda = 0.73$ Å radiation. Dynamic mechanical spectroscopy (DMS) experiments were performed using a Rheometrics Scientific ARES rheometer. All current samples in both the SAXS and DMS experiments were heated to temperatures exceeding the order−disorder transition before data were collected.

The ISO triblocks we investigated are labeled using the notation IS^xO^y, where x is the polydispersity index of the PS

* To whom correspondence should be addressed. E-mail: hillmyer@chem.umn.edu, bates@cems.umn.edu.
† Department of Chemical Engineering and Materials Science.
‡ Department of Chemistry.
§ These authors contributed equally to this work.

10.1021/ma071360a CCC: $37.00
Published on Web 08/29/2007

Table 1. ISO Characterization Data

polymer	PS M_n (kDa)	PS M_w/M_n	ISO M_n (kDa)	ISO M_w/M_n	N^a	$f_I{}^b$	$f_S{}^b$	$f_O{}^b$	phase[c]	T_{ODT} (°C)
$IS^{1.08}O^{0.10}$	7.3	1.08	15.2	1.05	234	0.45	0.45	0.10	LAM_2	164
$IS^{1.08}O^{0.13}$	7.3	1.08	15.8	1.05	242	0.44	0.44	0.13	O^{70}	194
$IS^{1.08}O^{0.15}$	7.3	1.08	16.3	1.05	249	0.42	0.43	0.15	O^{70}	217
$IS^{1.08}O^{0.18}$	7.3	1.08	16.9	1.06	256	0.41	0.41	0.18	O^{70}	246
$IS^{1.08}O^{0.21}$	7.3	1.08	17.8	1.06	268	0.39	0.40	0.21	O^{70}	267
$IS^{1.08}O^{0.24}$	7.3	1.08	18.5	1.05	278	0.38	0.38	0.24	O^{70}	292
$IS^{1.08}O^{0.27}$	7.3	1.08	19.4	1.06	289	0.36	0.37	0.27	LAM_3	>300
$IS^{1.31}O^{0.04}$	6.3	1.31	12.1	1.20	187	0.47	0.49	0.04	LAM	93
$IS^{1.31}O^{0.09}$	6.3	1.31	12.8	1.21	197	0.45	0.46	0.09	LAM	112
$IS^{1.31}O^{0.11}$	6.3	1.31	13.2	1.16	202	0.44	0.45	0.11	LAM	140
$IS^{1.31}O^{0.14}$	6.3	1.31	13.7	1.13	209	0.42	0.44	0.14	LAM	147
$IS^{1.31}O^{0.17}$	6.3	1.31	14.3	1.18	216	0.41	0.42	0.17	LAM	157
$IS^{1.31}O^{0.18}$	6.3	1.31	14.5	1.16	219	0.40	0.42	0.18	LAM	160
$IS^{1.31}O^{0.24}$	6.3	1.31	15.8	1.15	236	0.37	0.39	0.24	LAM	190
$IS^{1.31}O^{0.30}$	6.3	1.31	17.3	1.11	256	0.34	0.36	0.30	LAM	195
$IS^{1.44}O^{0.04}$	6.1	1.44	11.8	1.13	182	0.47	0.49	0.04	LAM	103
$IS^{1.44}O^{0.05}$	6.1	1.44	11.9	1.16	184	0.47	0.48	0.05	LAM	121
$IS^{1.44}O^{0.09}$	6.1	1.44	12.5	1.14	192	0.45	0.46	0.09	LAM	146
$IS^{1.44}O^{0.10}$	6.1	1.44	12.7	1.13	194	0.44	0.46	0.10	LAM	151
$IS^{1.44}O^{0.12}$	6.1	1.44	13.0	1.14	199	0.43	0.45	0.12	LAM	165
$IS^{1.44}O^{0.14}$	6.1	1.44	13.4	1.14	204	0.42	0.44	0.14	LAM	180
$IS^{1.44}O^{0.16}$	6.1	1.44	13.7	1.13	208	0.41	0.43	0.16	LAM	184
$IS^{1.44}O^{0.21}$	6.1	1.44	14.7	1.11	222	0.39	0.40	0.21	LAM[d]	216

[a] Based on a segment reference volume of 118 Å^3. [b] Volume fractions are calculated from published density values at 140 °C ($\rho_I = 0.830$, $\rho_S = 0.969$, $\rho_O = 1.064$ g/cm^3).[23] [c] Morphologies were identified using SAXS data. [d] A transient O^{70} morphology was identified in $IS^{1.44}O^{0.21}$ above 185 °C.

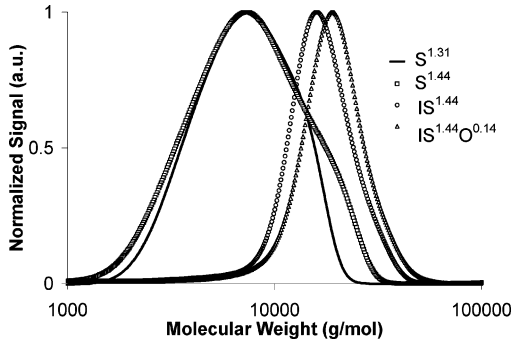

Figure 1. SEC traces of $S^{1.31}$, $S^{1.44}$, $IS^{1.44}$, and $IS^{1.44}O^{0.14}$. The molecular weight values used for the abscissa were obtained via calibration with PS standards.

block and *y* is the volume fraction of PEO (Table 1). The $IS^{1.08}O^y$ triblocks were previously synthesized,[17−19] and we measured $M_w/M_n = 1.08$ using SEC for PS after degradation of the PI in the $IS^{1.08}$ diblock via ozonolysis (toluene solution, −78 °C). The M_n values of the PS were determined using ^{1}H NMR end-group analysis, and these values agree to within 10% of those obtained from SEC. The composition and overall M_n of the ISO triblocks were determined using ^{1}H NMR spectroscopy. The volume fractions were calculated using experimental density values reported at 140 °C, and the *N* values correspond to a reference volume of 118 Å^3. The order−disorder transition temperatures were marked by a sharp drop in the dynamic elastic modulus upon heating the polymers at 1 °C/min[22] and in all cases were consistent with SAXS data.

SEC traces of $S^{1.31}$, $S^{1.44}$, $IS^{1.44}$, and $IS^{1.44}O^{0.14}$ are shown in Figure 1. The molecular weight values used for the abscissa were obtained via calibration with PS standards. The trace depicted for $IS^{1.44}$ was obtained after removal of the TIPS group; nearly identical data were collected for the polymer prior to deprotection, indicating that end-group effects were negligible. It is likely that the shape of the molecular weight distribution of the PS, and not just the M_w/M_n value, influences the morphological behavior of the resulting ISO triblocks.[24] Although that issue is not investigated here, the SEC data are presented with this idea in mind.

SAXS data collected at 120 °C for the $IS^{1.31}O^y$ triblocks are displayed on the right in Figure 2 alongside previously reported[19] SAXS data acquired at 160 °C for the $IS^{1.08}O^y$ triblocks. SAXS data are shown at different temperatures because three of the polydisperse samples ($IS^{1.31}O^{0.11}$, $IS^{1.31}O^{0.14}$, $IS^{1.31}O^{0.17}$) are disordered at 160 °C. None of these samples undergo order−order transitions prior to disordering, however, making these data representative of the morphologies adopted by the respective ISO triblocks. The difference in morphological behavior is evident upon comparison of these SAXS data. The $IS^{1.08}O^y$ triblocks adopt the orthorhombic network (O^{70}) (representative $IS^{1.08}O^{0.24}$ data are indexed to O^{70}) while the $IS^{1.31}O^y$ triblocks self-assemble into a lamellar morphology (representative $IS^{1.31}O^{0.30}$ data are indexed to lamellae). Similar SAXS data (not shown) were obtained for the $IS^{1.44}O^y$ triblocks, although a transient O^{70} morphology was identified above 185 °C in sample $IS^{1.44}O^{0.21}$. Two-domain lamellae (LAM_2) and three-domain lamellae (LAM_3) are not differentiated in the $IS^{1.31}O^y$ and $IS^{1.44}O^y$ triblocks as they were in the $IS^{1.08}O^y$ triblocks, where the O^{70} phase clearly separates the LAM_2 and LAM_3 morphologies.[17−19] The lack of an intermediate morphology in the $IS^{1.31}O^y$ and $IS^{1.44}O^y$ triblocks supports the notion of continuously varying composition profiles in the lamellar morphology. Such a continuous variation renders the distinction between LAM_2 and LAM_3 arbitrary, and all $IS^{1.31}O^y$ and $IS^{1.44}O^y$ lamellae are therefore denoted LAM (Table 1).

We propose two explanations for the altered morphological behavior brought about by the broadening of the PS molecular weight distribution. The first hypothesis follows directly from previous theoretical[8,10] and experimental[1,9] investigations which reported that block polydispersity increases the tendency of domain interfaces to curve toward the polydisperse block. This behavior has been attributed[1,9,10] to entropic effects associated with changes in chain stretching that are similar to those observed in conformationally asymmetric diblocks;[25] i.e., there is a tendency to curve an interface toward the polydisperse domain (lower stretching free energy) so that blocks in the

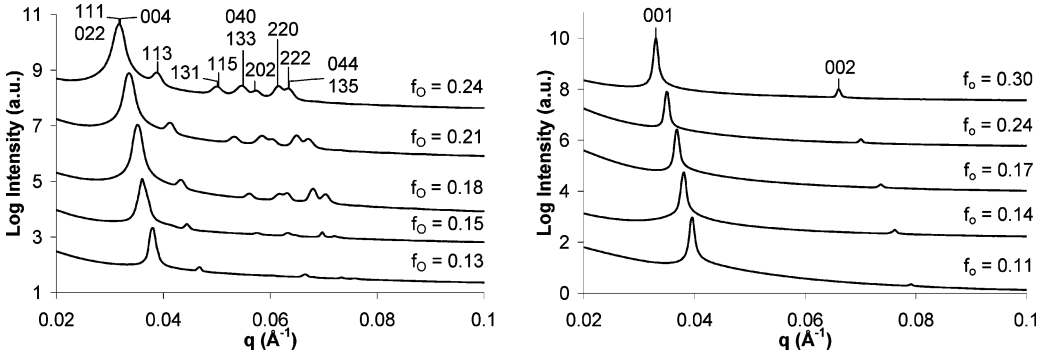

Figure 2. Synchrotron SAXS data for the $IS^{1.08}O^{y}$ and $IS^{1.31}O^{y}$ triblocks. The $IS^{1.08}O^{y}$ data presented in the plot on the left were acquired at 160 °C, and the $IS^{1.31}O^{y}$ data depicted in the plot on the right were acquired at 120 °C. None of these triblocks underwent order−order transitions prior to disordering. The representative $IS^{1.08}O^{0.24}$ and $IS^{1.31}O^{0.30}$ data are indexed to the O^{70} and LAM morphologies, respectively.

opposing domain may relax. In the O^{70} microstructure, both the I/S and S/O interfaces possess average mean curvature away from the PS domain. On the basis of this argument, curving the I/S and S/O interfaces toward the polydisperse PS domain will reduce constraints on chain conformations in a fashion analogous to the diblock case and result in a transformation of the morphology from O^{70} to lamellae.

A second explanation for the formation of lamellae instead of the O^{70} phase focuses on the required bridging of the PS block which is driven by a large χ_{IO} value. Network phases such as O^{70} and double gyroid do not have a uniform domain thickness. The variation in domain size leads to packing frustration as some polymer chains are excessively stretched (compressed), leading to an entropic penalty.[26] Broadening the molecular weight distribution of the center bridged block will exacerbate such packing frustration by requiring the shorter (longer) chains to stretch (compress) across the wide (narrow) portions of the domain; this entropic penalty may destabilize network morphologies. The critical polydispersity (PDI and overall distribution function) that destabilizes a network morphology presumably depends on the standard deviation of the mean curvature for that network; an M_w/M_n of 1.31 in the PS domain is apparently sufficient to destabilize O^{70} in ISO triblocks. It could be argued that polydispersity in the bridged domain would stabilize a network, with the longer chains segregating to the wider portions of the domain and the shorter chains localizing in the narrower sections of the domain. Such segregation by chain length would, however, result in a loss in overall translational entropy. A block copolymer could relieve the packing frustration without the accompanying loss in translational entropy by adopting a morphology with a uniform domain thickness (e.g., lamellae).

We have demonstrated that moderate polydispersity ($M_w/M_n = 1.31$) in a bridged domain can significantly alter the morphological behavior of triblock terpolymers. Unequivocally establishing the rationale for the formation of lamellae instead of the O^{70} network phase along the $f_I = f_S$ isopleth in ISO triblocks with a polydisperse PS domain requires further experimental and theoretical work. Elucidating the physical mechanism for this behavior will expand comprehension of polydispersity effects on the morphological behavior of block copolymers.

Acknowledgment. The authors gratefully acknowledge financial support from the Department of Energy through Grant 5-35908 and through a subcontract to UT-Battelle (No. 4000041622). We also acknowledge support from the National Science Foundation Materials Research Science and Engineering Center (NSF-MRSEC) at the University of Minnesota (NSF DMR-0212302). Graduate fellowships to A.J.M. from the Department of Homeland Security and the Department of Defense are gratefully acknowledged. Use of the Advanced Photon Source was supported by the U.S. Department of Energy, Basic Energy Sciences, Office of Science, under Contract W-31-109-Eng-38. Experiments were conducted at the research facilities of the DuPont-Northwestern-Dow Collaborative Access Team, which is supported by DuPont, Dow, NSF (DMR-9304725), and the Illinois Department of Commerce and Grant IBHE HECA NWU 96. The authors thank Dr. Cheng Lu for assistance with the ozonolysis and thank Nathaniel A. Lynd and Professor David C. Morse for helpful discussions.

References and Notes

(1) Ruzette, A.; Tence-Girault, S.; Leibler, L.; Chauvin, F.; Bertin, D.; Guerret, O.; Gerard, P. *Macromolecules* **2006**, *39*, 5804−5814.
(2) Leibler, L. *Macromolecules* **1980**, *13*, 1602−1617.
(3) Leibler, L.; Benoit, H. *Polymer* **1981**, *22*, 195−201.
(4) Hong, K. M.; Noolandi, J. *Polym. Commun.* **1984**, *25*, 265−268.
(5) Milner, S. T.; Witten, T. A.; Cates, M. E. *Macromolecules* **1989**, *22*, 853−861.
(6) Burger, C.; Ruland, W.; Semenov, A. N. *Macromolecules* **1990**, *23*, 3339−3346.
(7) Burger, C.; Ruland, W.; Semenov, A. N. *Macromolecules* **1991**, *24*, 816.
(8) Sides, S. W.; Fredrickson, G. H. *J. Chem. Phys.* **2004**, *121*, 4974−4986.
(9) Lynd, N. A.; Hillmyer, M. A. *Macromolecules* **2005**, *38*, 8803−8810.
(10) Cooke, D. M.; Shi, A. *Macromolecules* **2006**, *39*, 6661−6671.
(11) Matsen, M. W. *Eur. Phys. J. E* **2007**, *21*, 199−207.
(12) Matsushita, Y.; Noro, A.; Iinuma, M.; Suzuki, J.; Ohtani, H.; Takano, A. *Macromolecules* **2003**, *36*, 8074−8077.
(13) Noro, A.; Cho, D.; Takano, A.; Matsushita, Y. *Macromolecules* **2005**, *38*, 4371−4376.
(14) Noro, A.; Iinuma, M.; Suzuki, J.; Takano, A.; Matsushita, Y. *Macromolecules* **2004**, *37*, 3804−3808.
(15) Bendejacq, D.; Ponsinet, V.; Joanicot, M.; Loo, Y.-L.; Register, R. A. *Macromolecules* **2002**, *35*, 6645−6649.
(16) Frielinghaus, H.; Hermsdorf, N.; Almdal, K.; Mortensen, K.; Messe, L.; Corvazier, L.; Fairclough, J. P. A.; Ryan, A. J.; Olmsted, P. D.; Hamley, I. W. *Europhys. Lett.* **2001**, *53*, 680−686.
(17) Bailey, T. S.; Hardy, C. M.; Epps, T. H., III; Bates, F. S. *Macromolecules* **2002**, *35*, 7007−7017.
(18) Epps, T. H., III; Cochran, E. W.; Hardy, C. M.; Bailey, T. S.; Waletzko, R. S.; Bates, F. S. *Macromolecules* **2004**, *37*, 7085−7088.
(19) Epps, T. H., III; Cochran, E. W.; Bailey, T. S.; Waletzko, R. S.; Hardy, C. M.; Bates, F. S. *Macromolecules* **2004**, *37*, 8325−8341.
(20) Meuler, A. J.; Mahanthappa, M. K.; Hillmyer, M. A.; Bates, F. S. *Macromolecules* **2007**, *40*, 760−762.
(21) Hillmyer, M. A.; Bates, F. S. *Macromolecules* **1996**, *29*, 6994−7002.
(22) Rosedale, J. H.; Bates, F. S. *Macromolecules* **1990**, *23*, 2329−2338.
(23) Fetters, L. J.; Lohse, D. J.; Richter, D.; Witten, T. A.; Zirkel, A. *Macromolecules* **1994**, *27*, 4639−4647.
(24) Lynd, N. A.; Matsen, M. W. Personal communication, 2007.
(25) Matsen, M. W.; Bates, F. S. *J. Polym. Sci., Part B* **1997**, *35*, 945−952.
(26) Matsen, M. W.; Bates, F. S. *Macromolecules* **1996**, *29*, 7641−7644.

MA071360A